Progress In Electromagnetics Research, Vol. 128, 365–380, 2012

APPLICATION OF A USEFUL UNCERTAINTY ANALYSIS AS A METRIC TOOL FOR ASSESSING THE PERFORMANCE OF ELECTROMAGNETIC PROPERTIES RETRIEVAL METHODS OF BIANISOTROPIC METAMATERIALS

U. C. Hasar[1, 2, *], J. J. Barroso[3], M. Ertugrul[1, 2], C. Sabah[4], and B. Cavusoglu[1]

[1]Department of Electrical and Electronics Engineering, Ataturk University, Erzurum 25240, Turkey

[2]Center for Research and Application of Nanoscience and Nanoengineering, Ataturk University, Erzurum 25240, Turkey

[3]Associated Plasma Laboratory, National Institute for Space Research, São José dos Campos, SP 12227-010, Brazil

[4]Physikalisches Institut, J. W. Goethe Universität, Frankfurt, Germany

Abstract—We applied a useful uncertainty model, ignored in most metamaterials retrieval studies, to monitor the accuracy of retrieved electromagnetic properties of bianisotropic metamaterial (MM) slabs composed of split-ring resonators and cut wires. Two different MM slab structures are considered to make the analysis complete. As uncertainty-making factors, we took into consideration of uncertainties in scattering (S-) parameters of bianisotropic MM slabs as well as the length of these slabs. The applied uncertainty model is based upon considering the effect of minute change (differential) in uncertainty factors on the retrieved electromagnetic properties of bianisotropic MM slabs. The significant results concluded from the analysis are: 1) any abrupt changes in the phase of S-parameters of bianisotropic MM slabs remarkably influence the retrieved electromagnetic properties; 2) any small-scale loss (i.e., the loss of the substrate) in the bianisotropic MM slabs improves the accuracy of the retrieved electromagnetic properties of these slabs; and 3) precise knowledge of bianisotropic MM slab lengths are required for correct analysis of exotic properties

Received 8 April 2012, Accepted 23 May 2012, Scheduled 2 June 2012

* Corresponding author: Ugur Cem Hasar (ugur.hasar@yahoo.com).

of these slabs. The presented uncertainty analysis can be utilized as a metric tool for evaluating various retrieval methods of MM slabs in the literature.

1. INTRODUCTION

Metamaterials (MMs) have generated an enormous research interest in recent years for their ability to exhibit electromagnetic properties not found in conventional materials [1–6], such as a refractive index that is negative [7]. Loosely defined, a MM is an artificial crystal in which mesoscopic inclusion structures of natural materials are similar to artificial dielectrics obtained by arranging a large number of identical conducting obstacles, simulating the behavior of a molecule (or a group of molecules) in an ordinary dielectric, in a regular three-dimensional (3-D) pattern [8]. Fabricated MMs are composed of commonly metallic wire cuts and/or split-ring-resonators (SRRs). While metallic wire cut periodic array behaves like plasma and possesses a negative effective permittivity over a broadband, SRR periodic array produces a negative effective permeability within a limited frequency range [9].

There are some available methods in the literature for determining the electromagnetic properties of MMs [10–23]. While some of them are suitable for numerical simulations, others are appropriate for analytical models. Among these methods, S-parameters retrieval method is preferable for an analysis based on simulations as well as experimental point of view [10–31]. Depending on the wave polarization and its direction, MMs can exhibit bianisotropic property [11, 13, 15] and demonstrates unusual properties not found in normal isotropic MMs such as a wider stop-band in the transmission spectrum [11, 16], non-equal forward and backward wave impedances [11], and magnetoelectric coupling coefficient [11, 15]. Considering a survey over literature, to our best knowledge, we have noticed that most of the S-parameter extraction methods [10–13, 21–23] for determination of electromagnetic properties of MM slabs do not consider a complete analysis about the effect of increased uncertainty of measured S-parameters as well as slab length on the retrieved properties. As such, which retrieval method is best or appropriate for a specific analysis or problem is not clear. Although the retrieval method [21] discusses a sensitivity analysis for the effect of measured transmission S-parameter on the retrieved wave impedance of isotropic MM slabs, such an analysis, although it gives a clue, is not sufficient itself to monitor a complete picture of the dependence of measured S-parameters on retrieved electromagnetic properties. Besides, that analysis is not applicable to bianisotropic MMs. In this research

paper, we present how such a complete analysis can be performed using analytical expressions and then demonstrate the impact of increased uncertainty in measured/simulated S-parameters on the retrieved electromagnetic properties of bianisotropic MMs.

2. EXPRESSIONS OF SCATTERING PARAMETERS

The problem of determining effective electromagnetic properties of bianisotropic MMs with length d using forward and backward S-parameter measurements/simulations is depicted in Fig. 1.

The MM structures in Figs. 1(a) and 1(b) are excited by an electromagnetic wave with an electric field vector $\vec{E}$ oriented along x-axis, magnetic field vector $\vec{H}$ oriented along y-axis, and propagation vector $\vec{k}$ oriented along z-axis. Both of these structures have bianisotropic property since the electric field in the x direction induces a magnetic dipole in the y direction due to asymmetry of the inner and outer rings, while the magnetic field in the y direction also induces an electric dipole in the x direction [11, 15]. While the configuration in Fig. 1(a) is designated by the bianisotropic SRR MM, that in Fig. 1(b) is denoted by the bianisotropic Composite MM for the remainder part of our paper. By assuming that the harmonic time dependence is of the form $\exp(-i\omega t)$, implying that $n'' \geq 0$ (n is the refractive index) at all frequencies for passive media (throughout the paper, we use primes and double primes for denoting real and imaginary parts of a complex phasor quantity), and imposing boundary conditions of continuous electric and magnetic field transverse components at $z = 0$ and $z = d$ in Fig. 1, we derive the forward and backward reflection and transmission S-parameters of the homogeneous MM slabs in compact

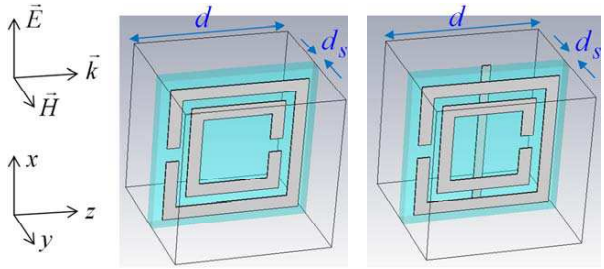

Figure 1. (a) Schematic of a single cell of a bianisotropic metamaterial with SRRs only and (b) schematic of a single cell of a bianisotropic metamaterial with SRRs and a wire.

form [14]

$$S_{11} = \frac{\Gamma_A\left(1-T^2\right)}{1-\Gamma_B T^2},\ S_{21}=S_{12}=\frac{\Gamma_C T}{1-\Gamma_B T^2},\ S_{22}=\frac{\Gamma_D\left(1-T^2\right)}{1-\Gamma_B T^2}, \quad (1)$$

$$\Gamma_A = \frac{z^+-1}{z^++1},\ \Gamma_B=\Gamma_A\Gamma_D,\ \Gamma_C=1-\Gamma_B,\ \Gamma_D=\frac{z^--1}{z^-+1}, \quad (2)$$

$$T = e^{ik_0nL},\ z^{\mp}=\frac{\mu_y}{n\mp i\xi_0},\ n=\mp\sqrt{\varepsilon_x\mu_y-\xi_0^2}. \quad (3)$$

for the constitutive parameters of each cell in Fig. 1

$$\overline{\overline{\varepsilon}} = \varepsilon_0\begin{pmatrix}\varepsilon_x & 0 & 0\\ 0 & \varepsilon_y & 0\\ 0 & 0 & \varepsilon_z\end{pmatrix},\quad \overline{\overline{\mu}}=\mu_0\begin{pmatrix}\mu_x & 0 & 0\\ 0 & \mu_y & 0\\ 0 & 0 & \mu_z\end{pmatrix}, \quad (4)$$

$$\overline{\overline{\xi}} = \frac{1}{c}\begin{pmatrix}0 & 0 & 0\\ 0 & 0 & 0\\ 0 & -i\xi_0 & 0\end{pmatrix},\quad \overline{\overline{\varsigma}}=\frac{1}{c}\begin{pmatrix}0 & 0 & 0\\ 0 & 0 & i\xi_0\\ 0 & 0 & 0\end{pmatrix}. \quad (5)$$

In Eqs. (1)–(5), z^+, z^-, n, and k_0 are, respectively, the normalized wave impedances in forward ($+z$) and backward ($-z$) directions and the refractive index of the bianisotropic MM slab, and free-space wave number; ε_x ε_y, ε_z, μ_x, μ_y, and μ_z are, respectively, the complex permittivity and complex permeability in x, y, and z directions; and ξ_0 is the magnetoelectric coupling coefficient. It is seen from Eqs. (1)–(3), for the wave propagation in z direction, only ε_x, μ_y, and ξ_0 are related to bianisotropic MM slabs in Fig. 1 [14]. In addition, $\overline{\overline{\xi}}$ and $\overline{\overline{\varsigma}}$ are interdependent, since for a lossless medium, $\overline{\overline{\xi}}$ is identical to the complex conjugate transpose of $\overline{\overline{\varsigma}}$, and in the case of a reciprocal medium, $\overline{\overline{\xi}}$ is equal to the negative transpose of $\overline{\overline{\varsigma}}$. Furthermore, as the rightmost term in Eq. (3) shows, for a bianisotropic MM slab, n (or the propagation wave vector) relates not only to ε_x and μ_y but also to ξ_0 [11]. In the retrieval of ε_x, μ_y, and ξ_0, as a first step, we eliminate T in S_{11} and S_{21} from Eq. (1), which produces a multiple-solutions set [28, 29]. As a second step, we substitute the found T into S_{22} and derive z^+ and z^-

$$z^+ = \frac{-\Lambda_2\mp\sqrt{\Lambda_2^2-4\Lambda_1\Lambda_3}}{2\Lambda_1},\quad z^-=\frac{\Lambda_4 z^++1}{z^++\Lambda_4}, \quad (6)$$

$$\Lambda_1 = S_{21}^2-(1-S_{11})(1-S_{22}),\quad \Lambda_2=2(S_{11}-S_{22}), \quad (7)$$

$$\Lambda_3 = (1+S_{11})(1+S_{22})-S_{21}^2,\quad \Lambda_4=\frac{S_{11}+S_{22}}{S_{11}-S_{22}}. \quad (8)$$

A complete description of the derivations in Eqs. (6)–(8) can be found in [14]. The correct sign for z^+ (and therefore z^-) can be assigned

considering that the bianisotropic MM slabs in Fig. 1 are passive ($z^{+'} > 0$). After determination of unique z^+ and z^- values from Eq. (6), we determine T from utilizing the expressions in Eq. (1)

$$T = \frac{\Gamma_A\left(1-\Gamma_B\right)S_{21}}{\Gamma_C\left(\Gamma_A - S_{11}\Gamma_B\right)} = \frac{\Gamma_D\left(1-\Gamma_B\right)S_{21}}{\Gamma_C\left(\Gamma_D - S_{22}\Gamma_B\right)}, \tag{9}$$

once upon incorporating the determined z^+ and z^- into Γ_A, Γ_B, Γ_C, and Γ_D in (2). Whereas the expression of T presented in [14] is two-valued, its new expression in Eq. (9) is single-valued, which is more feasible for retrieval of ε_x, μ_y, and ξ_0. Finally, we determine ε_x, μ_y, and ξ_0 parameters using Eq. (3)

$$n = \frac{1}{k_0 d}\left[\mp\left(\ln T\right)'' \mp 2\pi m - i\left(\ln T\right)'\right], \quad \xi_0 = \frac{\left(2-\Gamma_C\right)^2 - \left(4\Gamma_A^2 + \Gamma_C^2\right)}{4i\Gamma_A\Gamma_C/n}, \tag{10}$$

$$\mu_y = \frac{\Gamma_C\left(n^2+\xi_0^2\right)}{n\left(2-\Gamma_C\right) - 2n\Gamma_A - i\Gamma_C\xi_0}, \quad \varepsilon_x = \frac{n^2+\xi_0^2}{\mu_y}, \tag{11}$$

where $m = 0, 1, 2, 3, \ldots$, denotes the branch index value. It is seen from Eqs. (10) and (11) that the retrieved ε_x, μ_y, and ξ_0 have multiple solutions depending on m values. The correct choice of m for unique retrieval of ε_x, μ_y, and ξ_0 can be realized by different techniques [32–38].

3. SIMULATION RESULTS

We use the unit cell dimensions of [12] as for the dimensions of unit cells of our bianisotropic MM slabs in Fig. 1 to simulate S-parameters. Each unit cell in Fig. 1 is cubic with a cell dimension of $d = 2.5$ mm. The substrate with a thickness of $d_s = 0.25$ mm has a dielectric constant $\varepsilon_r = 4.4$ and a loss tangent of 0.0002. Perfect electric conductor (PEC) SRRs and wire, each has a thickness of 17 μm, are assumed positioned on opposite sides of the substrate. The width and height of the wire, respectively, are 0.14 mm and 2.5 mm. The outer ring length of the SRR is 2.2 mm and both rings have a linewidth of 0.2 mm. The gap opening in z direction in each ring is 0.3 mm, and the gap between the inner and outer rings is 0.15 mm. These unit cells are denoted as low-loss bianisotropic MM unit cells in the explanation of the results in our study. When the loss tangent of the substrate of MM slabs is increased to 0.02 and PEC of SRRs and wire is changed to copper with electrical conductivity 5.8×10^7 (S/m), the slabs are designated as lossy unit cells. We utilize the CST Microwave Studio simulation program based on finite integration technique [39] to simulate the S-parameters for each unit cell in Fig. 1. Whereas periodic boundary conditions

are used along x- and y-directions, waveguide ports are assumed along z-direction. For more details about the simulations, the reader can refer to [40]. For brevity, only the simulated S-parameters over $f = 7$–13 GHz of the low-loss unit cells are demonstrated in Figs. 2 and 3.

Note that because our formulation in Section 2 assumes a time dependence of $\exp(-i\omega t)$ while the CST software package considers the $\exp(+i\omega t)$ for its calculations, we negated the phase value of simulated S-parameters for the retrieval of electromagnetic properties in the remainder part of our study. Utilizing the expressions in (6)–(11) and simulated S-parameters, for each MM slab in Fig. 1, we first retrieve z^+, z^-, and n and then determine ε_x, μ_y, and ξ_0. For example, for the purpose of conciseness, we only demonstrate these parameters for the low-loss bianisotropic SRR and Composite MM slabs in Figs. 4–6.

It is seen from Fig. 4 that the dependencies of retrieved z^+ and z^- are in good agreement with those in [11]. It is noticed from Fig. 5(a) that the SRR MM slab has only positive n' over the frequency band while the Composite MM slab has a negative n' over some narrow

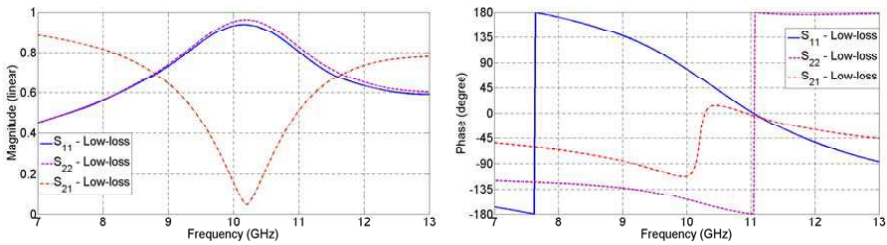

Figure 2. (a) Magnitude and (b) phase of the simulated S-parameters for the low-loss bianisotropic SRR MM cell.

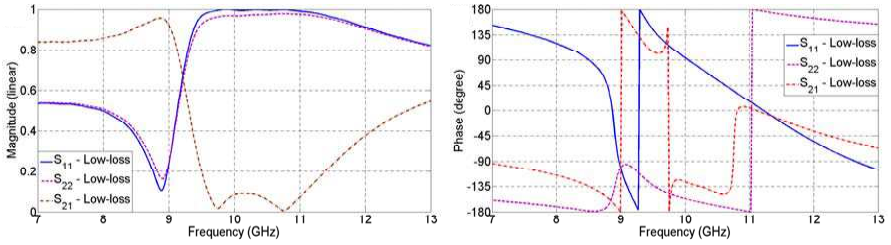

Figure 3. (a) Magnitude and (b) phase of the simulated S-parameters for the low-loss bianisotropic Composite MM cell.

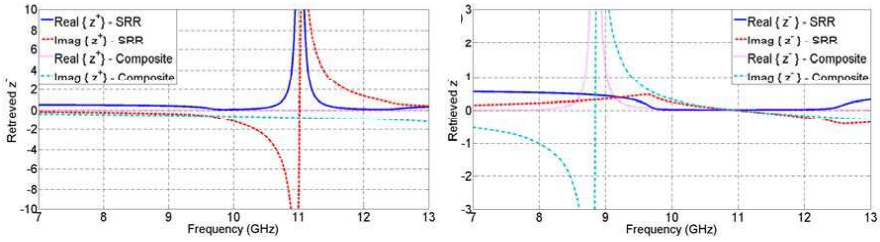

(a) (b)

Figure 4. Real and imaginary parts of retrieved (a) forward and (b) backward wave impedances of the low-loss bianisotropic SRR and Composite MM slabs.

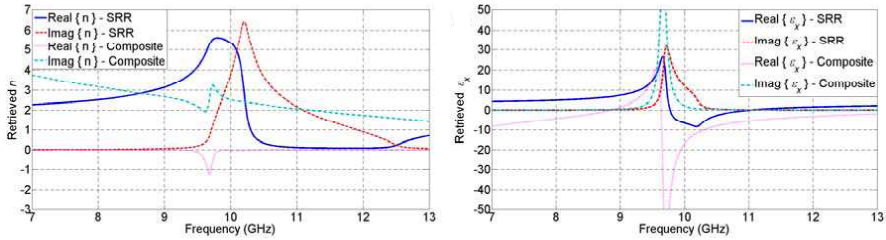

(a) (b)

Figure 5. Real and imaginary parts of retrieved (a) refractive index and (b) complex permittivity of the low-loss bianisotropic SRR and Composite MM slabs.

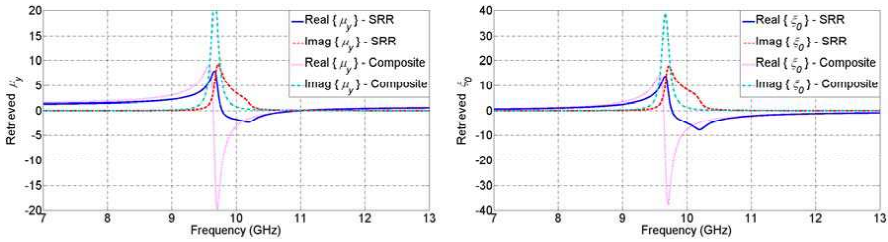

(a) (b)

Figure 6. Real and imaginary parts of retrieved (a) complex permeability and (b) magnetoelectric coupling coefficient of the low-loss bianisotropic SRR and Composite MM slabs.

frequency region (9.3–9.9 GHz). It is well-known that a MM structure composed of only SRRs cannot possess negative n' [10, 11]. We note from Figs. 5(b) and 6 that the retrieved ε'_x, μ'_y, and ξ'_0 for the SRR MM have all normal resonant behaviors and positive imaginary parts [11].

While the ξ_0' of our SRR MM has normal resonant behavior, that of the SRR MM in [11] (SRR-II in Fig. 3) shows antiresonant behavior, which is arising from the opposite direction of the wave propagation to the MM slab in [11]. Furthermore, it is seen from Figs. 5(b) and 6 that considering the retrieved ε_x, μ_y, and ξ_0, the SRR and Composite MM slabs share similar behaviors [11].

4. UNCERTAINTY ANALYSIS

In previous section, in the retrieval of electromagnetic properties, we assumed that there was no inaccuracy in the measured/simulated S-parameters. However, in practical applications, the magnitude and phase of each S-parameter have some inaccuracies associated with it [26–30]. In addition, measurements of MM slab lengths have some incorrectness even such measurements have been performed by a high precision micrometer, especially when the slab length decreases considerably. Furthermore, in most practical applications in the electromagnetic characterization of MM slabs, their thickness is arranged so that it is quite less than the operating wavelength in order to simplify the complexity of analysis (homogenous slab approach). As a result, it is evident that retrieved electromagnetic properties will be affected by the inaccuracies of S-parameter along with the slab length since these properties are interrelated with measured S-parameters and the slab length as seen in Eqs. (6)–(11).

After surveying some well-known proposed methods for the determination of electromagnetic properties of MM slabs [10, 11, 13, 21], we have noticed that these methods either did not consider at all or partially investigated the effect of the aforementioned inaccuracies on the retrieved electromagnetic properties of MM slabs. Therefore, it is difficult to evaluate not only the accuracy of proposed retrieval methods but also which retrieval method is suitable for a specific problem. A sensitivity analysis in [21] was performed so as to investigate the effect of measured transmission S-parameter on the retrieved wave impedance of isotropic MM slabs. It may give some insight on the accuracy of retrieved wave impedance. However, it is not a complete uncertainty analysis because it does not analyze the effect of S-parameter measurements on electromagnetic properties (not just wave impedance, but also permittivity, permeability, and so on) and because the analyzed sensitivity analysis in that paper cannot reflect the overall effect of inaccuracies of S-parameters as well as slab length on retrieved electromagnetic properties. Furthermore, it is evident that performing an uncertainty analysis for bianisotropic MMs is more difficult than that for isotropic MM slabs due to the increased complexity of S-parameter

expressions ($S_{11} \neq S_{22}$) in Eq. (1). To fill in this gap for electromagnetic characterization of bianisotropic MM slabs, in this research paper, we perform a full uncertainty analysis to assess the accuracy of retrieved ε_x, μ_y, and ξ_0. Toward this end, we utilize the well-known differential uncertainty model [26–28, 30, 41, 42], where the main factors contributing to the error budget are assumed $|S_{11}|$, $|S_{22}|$, $|S_{21}|$, θ_{11}, θ_{22}, θ_{21} and d. Here, the vertical bar and θ denote, respectively, the magnitude and phase of the corresponding complex quantity. Following the procedure in [42], we find

$$\frac{\Delta\chi}{\chi} = \frac{1}{\chi}\sqrt{\sum_u \left[\left(\frac{\partial\chi}{\partial|S_u|}\Delta|S_u|\right)^2 + \left(\frac{\partial\chi}{\partial\theta_u}\Delta\theta_u\right)^2\right] + \left(\frac{\partial\chi}{\partial d}\Delta d\right)^2}, \quad (12)$$

where χ stands for ε_x, μ_y, or ξ_0 and $u = 11$, 22, and 21. The explicit expressions of partial derivatives in Eq. (12) are given below for the purpose that our presented uncertainty analysis can be used as a tool for assessing different retrieval methods in the literature

$$\frac{\partial\varepsilon_x}{\partial|S_{11}|} = \frac{\Omega_6 h_1 e^{i\theta_{11}}}{h_1h_2 + h_3h_4}, \quad \frac{\partial\mu_y}{\partial|S_{11}|} = \frac{h_4}{h_1}\frac{\partial\varepsilon_x}{\partial|S_{11}|},$$
$$\frac{\partial\xi_0}{\partial|S_{11}|} = -\left(\frac{\Omega_4}{\Omega_6}\frac{\partial\varepsilon_x}{\partial|S_{11}|} + \frac{\Omega_5}{\Omega_6}\frac{\partial\mu_y}{\partial|S_{11}|}\right), \quad (13)$$

$$\frac{\partial\varepsilon_x}{\partial|S_{21}|} = \frac{\Omega_3 h_3 e^{i\theta_{21}}}{h_2h_5 + h_3h_6}, \quad \frac{\partial\mu_y}{\partial|S_{21}|} = \frac{-h_2}{h_3}\frac{\partial\varepsilon_x}{\partial|S_{21}|},$$
$$\frac{\partial\xi_0}{\partial|S_{21}|} = -\left(\frac{\Omega_1}{\Omega_3}\frac{\partial\varepsilon_x}{\partial|S_{21}|} + \frac{\Omega_2}{\Omega_3}\frac{\partial\mu_y}{\partial|S_{21}|}\right), \quad (14)$$

$$\frac{\partial\varepsilon_x}{\partial|S_{22}|} = \frac{-\Omega_3 h_5 e^{i\theta_{22}}}{h_2h_5 + h_3h_6}, \quad \frac{\partial\mu_y}{\partial|S_{22}|} = \frac{h_6}{h_5}\frac{\partial\varepsilon_x}{\partial|S_{22}|},$$
$$\frac{\partial\xi_0}{\partial|S_{22}|} = -\left(\frac{\Omega_1}{\Omega_3}\frac{\partial\varepsilon_x}{\partial|S_{22}|} + \frac{\Omega_2}{\Omega_3}\frac{\partial\mu_y}{\partial|S_{22}|}\right), \quad (15)$$

$$\frac{\partial\varepsilon_x}{\partial d} = \frac{h_3h_7 - h_5h_8}{h_3h_6 + h_1h_5}, \quad \frac{\partial\mu_y}{\partial d} = -\frac{h_7}{h_5} + \frac{h_6}{h_5}\frac{\partial\varepsilon_x}{\partial d},$$
$$\frac{\partial\xi_0}{\partial d} = \frac{\Omega_{10}}{\Omega_3} - \left(\frac{\Omega_1}{\Omega_3}\frac{\partial\varepsilon_x}{\partial d} + \frac{\Omega_2}{\Omega_3}\frac{\partial\mu_y}{\partial d}\right), \quad (16)$$

$$\frac{\partial\chi}{\partial\theta_{11}} = i|S_{11}|\frac{\partial\chi}{\partial|S_{11}|}, \quad \frac{\partial\chi}{\partial\theta_{21}} = i|S_{21}|\frac{\partial\chi}{\partial|S_{21}|}, \quad \frac{\partial\chi}{\partial\theta_{22}} = i|S_{22}|\frac{\partial\chi}{\partial|S_{22}|}, \quad (17)$$

$$h_1 = \Omega_5\Omega_9 - \Omega_6\Omega_8, \quad h_2 = \Omega_1\Omega_6 - \Omega_3\Omega_4, \quad h_3 = \Omega_2\Omega_6 - \Omega_3\Omega_5,$$
$$h_4 = \Omega_6\Omega_7 - \Omega_4\Omega_9, \quad (18)$$

$$h_5 = \Omega_2\Omega_9 - \Omega_3\Omega_8, \quad h_6 = \Omega_3\Omega_7 - \Omega_1\Omega_9, \quad h_7 = \Omega_3\Omega_{12} - \Omega_9\Omega_{10},$$
$$h_8 = \Omega_3\Omega_{11} - \Omega_6\Omega_{10}, \tag{19}$$

$$\Omega_t = \left(\frac{\partial S_{11}}{\partial \Gamma_A}\frac{\partial \Gamma_A}{\partial z^+} + \frac{\partial S_{11}}{\partial \Gamma_B}\frac{\partial \Gamma_B}{\partial z^+}\right)\frac{\partial z^+}{\partial \chi} + \frac{\partial S_{11}}{\partial \Gamma_B}\frac{\partial \Gamma_B}{\partial z^-}\frac{\partial z^-}{\partial \chi} + \frac{\partial S_{11}}{\partial T}\frac{\partial T}{\partial \chi}, \tag{20}$$

$$\Omega_{(t+3)} = \frac{\partial S_{22}}{\partial \Gamma_B}\frac{\partial \Gamma_B}{\partial z^+}\frac{\partial z^+}{\partial \chi} + \left(\frac{\partial S_{22}}{\partial \Gamma_B}\frac{\partial \Gamma_B}{\partial z^-} + \frac{\partial S_{22}}{\partial \Gamma_D}\frac{\partial \Gamma_D}{\partial z^-}\right)\frac{\partial z^-}{\partial \chi} + \frac{\partial S_{22}}{\partial T}\frac{\partial T}{\partial \chi}, \tag{21}$$

$$\Omega_{(t+6)} = \left(\frac{\partial S_{21}}{\partial \Gamma_B}\frac{\partial \Gamma_B}{\partial z^+} + \frac{\partial S_{21}}{\partial \Gamma_C}\frac{\partial \Gamma_C}{\partial z^+}\right)\frac{\partial z^+}{\partial \chi} + \left(\frac{\partial S_{21}}{\partial \Gamma_B}\frac{\partial \Gamma_B}{\partial z^-} + \frac{\partial S_{21}}{\partial \Gamma_C}\frac{\partial \Gamma_C}{\partial z^-}\right)\frac{\partial z^-}{\partial \chi} + \frac{\partial S_{21}}{\partial T}\frac{\partial T}{\partial \chi}, \tag{22}$$

$$\Omega_{10} = -\frac{\partial S_{11}}{\partial T}\frac{\partial T}{\partial d}, \quad \Omega_{11} = -\frac{\partial S_{22}}{\partial T}\frac{\partial T}{\partial d}, \quad \Omega_{12} = -\frac{\partial S_{21}}{\partial T}\frac{\partial T}{\partial d}. \tag{23}$$

In (20)–(22), $t = 1$, 2, or 3. It is assumed that the functions in Eqs. (12)–(22) are analytic (differentiable) over the region of interest with respect to the differentiation variables [42]. For evaluating the explicit expressions in Eq. (12), we first consider the simulated S-parameters of the low-loss and lossy SRR and Composite MM slabs. Then, we apply our proposed retrieval method and draw the dependence of $\Delta\chi/\chi$ over frequency. For example, Figs. 7 and 8(a) demonstrate the dependence of $\Delta\varepsilon_x/\varepsilon_x$, $\Delta\mu_y/\mu_y$, and $\Delta\xi_0/\xi_0$ over $f = 7$–13 GHz for the low-loss and lossy Composite MM slabs which the latter shows negative n. Here, the errors due to S-parameters are taken as $\Delta|S_{11}| = \Delta|S_{21}| = \Delta|S_{22}| = 0.0025$ and $\Delta\theta_{11} = \Delta\theta_{21} = \Delta\theta_{22} = 0.025°$, and $\Delta d = 0$.

It is seen from Figs. 7 and 8(a) that the uncertainty in the ε'_x, μ'_y, and ξ'_0 determination drastically increases at some specific

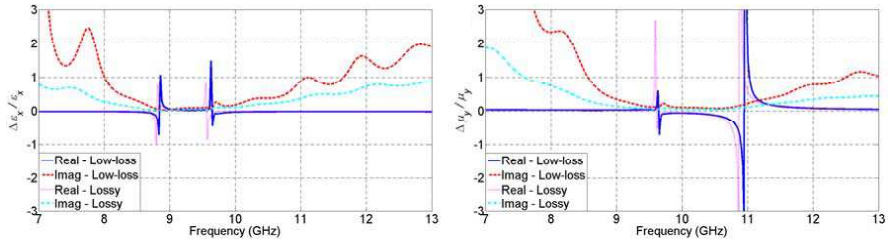

Figure 7. Frequency dependence of the real and imaginary parts of (a) the $\Delta\varepsilon_x/\varepsilon_x$ and (b) the $\Delta\mu_y/\mu_y$ for the low-loss and lossy Composite MM slabs.

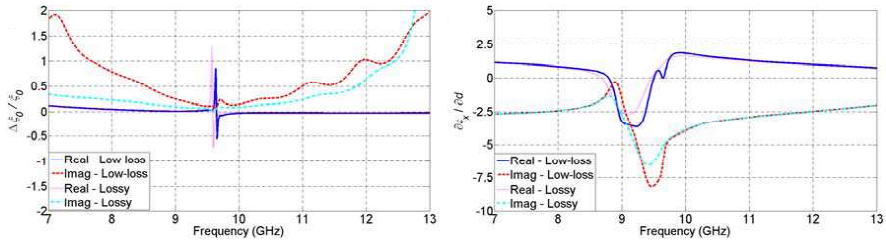

Figure 8. Frequency dependence of the real and imaginary parts of (a) the $\Delta\xi_0/\xi_0$ and (b) the $\partial\varepsilon_x/\partial d$ for the low-loss and lossy Composite MM slabs.

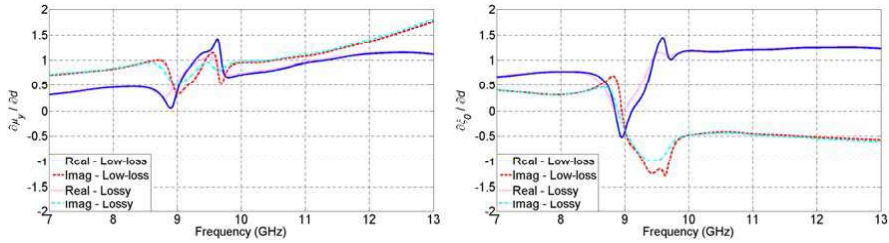

Figure 9. Frequency dependence of the real and imaginary parts of (a) the $\partial\mu_y/\partial d$ and (b) the $\partial\xi_0/\partial d$ for the low-loss and lossy Composite MM slabs.

frequency points. At those frequencies, the retrieved electromagnetic properties are not much reliable [26–28]. For example, the dependence of $\Delta\varepsilon'_x/\varepsilon'_x$ for the low-loss Composite MM slab has two sharp peaks at $f \cong 8.84\,\text{GHz}$ and $f \cong 9.64\,\text{GHz}$. These peaks, respectively, correspond to the regions where the z^- and n change drastically in Figs. 4(b) and 5(a). The dependence of $\Delta\mu'_y/\mu'_y$ for the low-loss Composite MM slab has also two large changes at $f \cong 9.64\,\text{GHz}$ and $f \cong 10.95\,\text{GHz}$, corresponding, respectively, to the regions where n has a drastic change in Fig. 5(a) and where θ_{21} suddenly increases by jumping to a peak at around 10.9 GHz in Fig. 3(b). Besides, the dependence of $\Delta\xi'_0/\xi'_0$ for the low-loss Composite MM slab has only one significant change at $f \cong 9.64\,\text{GHz}$. This frequency coincides with the region where n has a drastic change in Fig. 5(a). On the other hand, it is noted from Figs. 7 and 8(a) that $\Delta\varepsilon''_x/\varepsilon''_x$, $\Delta\mu''_y/\mu''_y$, and $\Delta\xi''_0/\xi''_0$ have smoother dependences over the frequency band. From these results, we draw two conclusions. First, any abrupt changes in the measured θ_{11}, θ_{22}, and

θ_{21} (especially resonant region of the MM slabs) over frequency make difficult to determine the accurate value of ε_x', μ_y', and ξ_0', although there is no physical phase discontinuity (phases can be unwrapped by [38]), since our uncertainty model assumes that all the dependent variables are continuous and considers differential uncertainty concept so that any fast change in a parameter produces a larger change in its uncertainty. Second, an increase in the overall loss of the MM slab facilitates the correct determination of ε_x'', μ_y'', and ξ_0'' for medium-loss or lossy materials.

For the dependencies in Figs. 7 and 8(a), we considered $\Delta d = 0$. Now we focus on monitoring the dependences of $\partial\varepsilon_x/\partial d$, $\partial\mu_y/\partial d$, and $\partial\xi_0/\partial d$ over frequency. Toward this end, we obtain $\partial\varepsilon_x/\partial d$, $\partial\mu_y/\partial d$, and $\partial\xi_0/\partial d$ (the value of Δd depends on how accurately the slab is prepared and therefore is dependent upon the operator) over frequency as shown in Figs. 8(b) and 9. It is seen from Figs. 8(b) and 9 that the dependencies of $\partial\varepsilon_x/\partial d$, $\partial\mu_y/\partial d$, and $\partial\xi_0/\partial d$ over frequency have almost a minor but stable variation except for the frequency region over 8.4–9.8 GHz. This frequency region corresponds to the resonance of the low-loss and lossy Composite MM slabs, as can be seen from Fig. 5(a). In addition, it is seen from Figs. 8(a) and 9 that the impact of MM slab losses mainly alters the dependencies of $\partial\varepsilon_x/\partial d$, $\partial\mu_y/\partial d$, and $\partial\xi_0/\partial d$ near resonance frequencies, which indicates that accurate knowledge of MM slab length is a prerequisite for accurate retrieval of exotic electromagnetic properties of MM slabs such as negative n. The dependencies of $\Delta\varepsilon_x/\varepsilon_x$, $\Delta\mu_y/\mu_y$, $\Delta\xi_0/\xi_0$, $\partial\varepsilon_x/\partial d$, $\partial\mu_y/\partial d$, and $\partial\xi_0/\partial d$ for the low-loss and lossy bianisotropic SRR MM slabs are similar to those of the low-loss and lossy bianisotropic Composite MM slabs, since the extracted ε_x, μ_y, and ξ_0 values for both MM slabs resemble. Therefore, these dependencies are not given here for conciseness.

5. CONCLUSION

In this research paper, we have performed a complete uncertainty analysis to assess the correctness of retrieved electromagnetic properties of bianisotropic MM slabs. Two different types of slab configurations composed of only SRR (SRR MM slab) and of SRR and a wire cut (Composite MM slab), as well as their different loss properties are utilized for this purpose. To demonstrate the dependencies of extracted electromagnetic properties on uncertainty factors, we first presented the explicit expressions of these properties. As uncertainty factors, we considered the uncertainties in S-parameters of bianisotropic SRR and Composite MM slabs as well as the length

of these slabs. Then, we applied an uncertainty model (differential uncertainty model) and derived closed-form expressions of uncertainty terms to be used in the model. From the analysis, we concluded three important results. First, we noticed that any sharp changes in the phase of S-parameters of bianisotropic SRR and Composite MM slabs notably affect the retrieved electromagnetic properties. Second, any loss present in the bianisotropic SRR and Composite MM slabs, arising from the loss of the substrate and finite electrical conductivity of SRRs and wire cuts in a cell, allows accurate retrieval of electromagnetic properties of these slabs, provided that this loss does not suppress the resonance behavior of MM slabs and is not considerably high to influence the uncertainty in transmission S-parameter. Third, for accurate retrieval of unusual properties of bianisotropic SRR and Composite MM slabs such as negative n, precise knowledge of their slab lengths is needed.

REFERENCES

1. Veselago, V. G., "The electrodynamics of substances with simultaneously negative values of ε and μ," *Sov. Phys. USPEKHI*, Vol. 10, 509–514, 1968.
2. Pendry, J. B., "Negative refraction makes a perfect lens," *Phys. Rev. Lett.*, Vol. 85, 3966–3969, 2000.
3. Shelby, R. A., D. R. Smith, and S. Shultz, "Experimental verification of a negative index of refraction," *Science*, Vol. 292, 77–79, 2001.
4. Duan, Z., B.-I. Wu, S. Xi, H. Chen, and M. Chen, "Research progress in reversed Cherenkov radiation in double-negative metamaterials," *Progress In Electromagnetics Research*, Vol. 90, 75–87, 2009.
5. Cojocaru, E., "Electromagnetic tunneling in lossless trilayer stacks containing single-negative metamaterials," *Progress In Electromagnetics Research*, Vol. 113, 227–249, 2011.
6. Oraizi, H., A. Abdolali, and N. Vaseghi, "Application of double zero metamaterials as radar absorbing materials for the reduction of radar cross section," *Progress In Electromagnetics Research*, Vol. 101, 323–337, 2010.
7. Jiang, Z. H., J. A. Bossard, X. Wang, and D. H. Werner, "Synthesizing metamaterials with angularly independent effective medium properties based on an anisotropic parameter retrieval technique coupled with a genetic algorithm," *J. Appl. Phys.*, Vol. 109, 013515, 2011.

8. Collin, R. E., *Field Theory of Guided Waves*, Wiley-IEEE Press, 1990.
9. Koschny, T., M. Kafesaki, E. N. Economou, and C. M. Soukolis, "Effective medium theory of left-handed materials," *Phys. Rev. Lett.*, Vol. 93, 107402, 2004.
10. Smith, D. R., S. Schultz, P. Markos, and C. M. Soukoulis, "Determination of effective permittivity and permeability of metamaterials from reflection and transmission coefficients," *Phys. Rev. B*, Vol. 65, 195104, 2002.
11. Li, Z., K. Aydin, and E. Ozbay, "Determination of the effective constitutive parameters of bianisotropic metamaterials from reflection and transmission coefficients," *Phys. Rev. E*, Vol. 79, 026610, 2009.
12. Smith, D. R., D. C. Vier, T. Koschhy, and C. M. Soukoulis, "Electromagnetic parameter retrieval from inhomogeneous metamaterials," *Phys. Rev. E*, Vol. 71, 036617, 2005.
13. Chen, X., B.-I. Wu, J. A. Kong, and T. M. Grzegorczyk, "Retrieval of the effective constitutive parameters of bianisotropic metamaterials," *Phys. Rev. E*, Vol. 71, 046610, 2005.
14. Hasar, U. C. and J. J. Barroso, "Retrieval approach for determination of forward and backward wave impedances of bianisotropic metamaterials," *Progress In Electromagnetics Research*, Vol. 112, 109–124, 2011.
15. Marques, R., F. Medina, and R. Rafii-El-Idrissi, "Role of bianisotropy in negative permeability and left-handed metamaterials," *Phys. Rev. B*, Vol. 65, 144440, 2002.
16. Katsarakis, N., T. Koschny, M. Kafesaki, E. N. Economou, and C. M. Soukoulis, "Electric coupling to the magnetic resonance of split ring resonators," *Appl. Phys. Lett.*, Vol. 84, 2943–2945, 2004.
17. Alu, A., "First-principles homogenization theory for periodic metamaterials," *Phys. Rev. B*, Vol. 84, 075153, 2011.
18. Lubrowski, G., R. Schuhmann, and T. Weiland, "Extraction of effective metamaterial parameters by parameter fitting of dispersive models," *Microw. Opt. Technol. Lett.*, Vol. 49, 285–288, 2007.
19. Markos, P. and C. M. Soukoulis, "Transmission properties and effective electromagnetic parameters of double negative metamaterials," *Opt. Express*, Vol. 11, 649–661, 2003.
20. Ziolkowski, R. W., "Design, fabrication, and testing of double negative metamaterials," *IEEE Trans. Antennas Propag.*, Vol. 51, 1516–1529, 2003.

21. Chen, X., T. M. Grzegorczyk, B.-I. Wu, J. Pacheco, Jr., and J. A. Kong, "Robust method to retrieve the constitutive effective parameters of metamaterials," *Phys. Rev. E*, Vol. 70, 016608, 2004.
22. Andryieuski, A., R. Malureanu, and A. V. Lavrinenko, "Wave propagation retrieval method for chiral metamaterials," *Opt. Express*, Vol. 18, No. 15, 15498–15503, 2010.
23. Andryieuski, A., C. Menzel, C. Rockstuhl, R. Malureanu, F. Lederer, and A. Lavrinenko, "Homogenization of resonant chiral metamaterials," *Phys. Rev. B*, Vol. 82, 235107, 2010.
24. Nicolson, A. M. and G. Ross, "Measurement of the intrinsic properties of materials by time-domain techniques," *IEEE Trans. Instrum. Meas.*, Vol. 19, 377–382, 1970.
25. Weir, W. B., "Automatic measurement of complex dielectric constant and permeability at microwave frequencies," *Proc. IEEE*, Vol. 62, 33–36, 1974.
26. Baker-Jarvis, J., E. J. Vanzura, and W. A. Kissick, "Improved technique for determining complex permittivity with the transmission/reflection method," *IEEE Trans. Microw. Theory Tech.*, Vol. 38, 1096–1103, 1990.
27. Boughriet, A. H., C. Legrand, and A. Chapoton, "Noniterative stable transmission/reflection method for low-loss material complex permittivity determination," *IEEE Trans. Microw. Theory Tech.*, Vol. 45, 52–57, 1997.
28. Hasar, U. C. and C. R. Westgate, "A broadband and stable method for unique complex permittivity determination of low-loss materials," *IEEE Trans. Microw. Theory Tech.*, Vol. 57, 471–477, 2009.
29. Barroso, J. J. and A. L. de Paula, "Retrieval of permittivity and permeability of homogeneous materials from scattering parameters," *Journal of Electromagnetic Waves and Applications*, Vol. 24, Nos. 11–12, 1563–1574, 2010.
30. Chalapat, K., K. Sarvala, J. Li, and G. S. Paraoanu, "Wideband reference-plane invariant method for measuring electromagnetic parameters of materials," *IEEE Trans. Microw. Theory Tech.*, Vol. 57, 2257–2267, 2009.
31. Hasar, U. C. and Y. Kaya, "Reference-independent microwave method for constitutive parameters determination of liquid materials from measured scattering parameters," *Journal of Electromagnetic Waves and Applications*, Vol. 25, Nos. 11–12, 1708–1717, 2011.

32. Weir, W. B., "Automatic measurement of complex dielectric constant and permeability at microwave frequencies," *Proc. IEEE*, Vol. 62, 33–36, 1974.
33. Muqaibel, A. H. and A. Safaai-Jazi, "A new formulation for characterization of materials based on measured insertion transfer function," *IEEE Trans. Microw. Theory Tech.*, Vol. 51, 1946–1951, 2003.
34. Xia, S., Z. Xu, and X. Wei, "Thickness-induced resonance-based complex permittivity measurement technique for barium strontium titanate ceramics at microwave frequency," *Rev. Sci. Instrum.*, Vol. 80, 114703, 2009.
35. Buyukozturk, O., T.-Y. Yu, and J. A. Ortega, "A methodology for determining complex permittivity of construction materials based on transmission-only coherent, wide-bandwidth free-space measurements," *Cem. Concr. Compos.*, Vol. 28, 349–359, 2006.
36. Szabo, Z., G.-H. Park, R. Hedge, and E.-P. Li, "Unique extraction of metamaterial parameters based on Kramers-Kronig relationship," *IEEE Trans. Microw. Theory Tech.*, Vol. 58, 2646–2653, 2010.
37. Varadan, V. V. and R. Ro, "Unique retrieval of complex permittivity and permeability of dispersive materials from reflection and transmitted fields by enforcing causality," *IEEE Trans. Microw. Theory Tech.*, Vol. 55, 2224–2230, 2007.
38. Barroso, J. J. and U. C. Hasar, "Resolving phase ambiguity in the inverse problem of transmission/reflection measurement methods," *Int. J. Infrared Milli. Waves*, Vol. 32, 857–866, 2011.
39. Weiland, T., R. Schuhmann, R. B. Greegor, C. G. Parazzoli, A. M. Vetter, D. R. Smith, D. C. Vier, and S. Schultz, "Ab *initio* numerical simulation of left-handed metamaterials: Comparison of calculations and experiments," *J. Appl. Phys.*, Vol. 90, 5419–5424, 2001.
40. Lubkowski, G., B. Bandlow, R. Schuhmann, and T. Weiland, "Effective modeling of double negative metamaterial macrostructures," *IEEE Trans. Microw. Theory Tech.*, Vol. 57, 1136–1146, 2009.
41. Kline, S. J. and F. A. McClintock, "Describing uncertainties in single-sample experiments," *Mech. Eng.*, Vol. 75, 3, 1953.
42. Baker-Jarvis, J., M. D. Janezic, J. H. Grosvenor, Jr., and R. G. Geyer, "Transmission/reflection and short-circuit line methods for measuring permittivity and permeability," Tech. Note 1355, NIST, Boulder, CO, 1992.